A&A 444, 347–355 (2005)
DOI: 10.1051/0004-6361:20042603

Astronomy & Astrophysics

Convective magneto-rotational instabilities in accretion disks

E. van der Swaluw, J. W. S. Blokland⋆, and R. Keppens⋆

FOM-Institute for Plasma Physics Rijnhuizen, PO Box 1207, 3430 BE Nieuwegein, The Netherlands
e-mail: swaluw@rijnh.nl

Received 23 December 2004 / Accepted 13 April 2005

ABSTRACT

We present a study of instabilities occuring in thick magnetized accretion disks. We calculate the growth rates of these instabilities and characterise precisely the contribution of the magneto-rotational and convective mechanism. All our calculations are performed in radially stratified disks in the cylindrical limit. The numerical calculations are performed using the appropriate local dispersion equation solver discussed in Blokland et al. (2005, A&A, 444, 337). A comparison with recent results by Narayan et al. (2002, ApJ, 577, 295) shows excellent agreement with their approximate growth rates only if the disks are weakly magnetized. However, for disks close to equipartition, the dispersion equation from Narayan et al. (2002) loses its validity. Our calculations allow for quantitative determination of the increase in growth rate due to the magneto-rotational mechanism. We find that the increase of the growth rate for long wavelength convective modes caused by this mechanism is almost neglible. On the other hand, the growth rate of short wavelength instabilities can be significantly increased by this mechanism, reaching values up to 60%.

Key words. accretion, accretion disks – instabilities – magnetohydrodynamics (MHD) – plasmas

1. Introduction

Accretion disks are present around a variety of astrophysical objects, ranging from young proto-stars in star formation regions to massive black holes in the centres of galaxies. A standard model of a geometrically thin accretion disk was introduced in the early seventies by Shakura & Sunyaev (1973). In their model, angular momentum is transported outwards by an anomalous viscosity mechanism, which is parametrised by the α-parameter. This parameter scales linearly with the radial-azimuthal component of the stress tensor, which is associated with the viscous torque that provides the angular momentum transport. The assumption of a geometrically thin disk implies that the gravitational energy release by viscous dissipation is locally radiated away.

It was realised in the early nineties that the anomalous viscosity mechanism can be provided by the turbulence that arises from the magneto-rotational instability (Balbus & Hawley 1991). These authors showed that this essentially magnetic instability is a very robust one that occurs in weakly magnetized thin accretion disks.

However, in recent years, Chandra observations have found examples of underluminous black holes at X-ray frequencies. A good example is our own Galactic Centre, Sgr A* (Baganoff et al. 2001), and the galactic centre of the elliptic galaxy M 87 (Di Matteo et al. 2003). These observations might be explained in the context of nonradiating accretion flows, which are still using the α description from Shakura & Sunyaev (1973), but are no longer geometrically thin (Narayan & Li 1994). One of these models that has gained a lot of interest in the literature in recent years is the convection-dominated accretion flow (CDAF). In this type of accretion flow models, the transport of the angular momentum outwards by the turbulence arising from the magneto-rotational instability is partly counterbalanced by transport inwards due to convective motion occuring in these *thick* accretion disks. Therefore the accretion rate might be efficiently reduced, which might explain the lower observed X-ray luminosities in Sgr A* and the central region of M 87.

Recent studies of these CDAF-type of disks, in which both convective and magneto-rotational instabilities can be found, have been performed by Balbus & Hawley (2002) and Narayan et al. (2002). These authors have used a linear stability analysis and identified unstable long-wavelength modes with a convective nature, and short-wavelength modes with a more dominant MRI behaviour.

In this paper, we elaborate on the work of Narayan et al. (2002). These authors have considered a differentially rotating and thermally stratified plasma with a weak axial magnetic field. They use the equation for the growth rate obtained by Balbus & Hawley (1991), who used linear stability theory to derive it. Narayan et al. (2002) consider five models of an accretion disk, each with a different value of the assumed uniform Brunt-Väisälä frequency. Their results clearly show the rise of a plateau in the obtained growth rate at low axial wavenumbers as the Brunt-Väisälä frequency is increased. They argue that the modes in this plateau are identified as convective modes, once

⋆ Association EURATOM-FOM, Trilateral Euregio Cluster.

the Brunt-Väisälä frequency exceeds the epicyclic frequency, i.e. the Høiland criterion (Tassoul 1987). The exact nature of a mode in this plateau is identified using results from the linear stability theory as performed by Balbus & Hawley (1991, 2002).

We follow up on the above-mentioned work, but we numerically solve a sixth order polynomial dispersion relation, using the Local Dispersion Equation Solver (LODES), which was already discussed in Blokland et al. (2005). We will not only consider weakly magnetized disks, but also consider models which are closer to equipartition. We consider a differentially rotating plasma for which the equilibrium quantities are power-law profiles of the radius. Furthermore, we explicitly define a value for the scale height of the disk H with respect to the radius r using the free parameter $\epsilon = H/r$.

In our present analysis we only consider axisymmetric perturbations, which means that in a model with a purely toroidal magnetic field, the magneto-rotational mechanism is excluded. Therefore in such models, the obtained modes are purely convective. The growth rates from these modes can be compared to a similar model that includes a *weak* axial magnetic field. This enables one to observe the increase in growth rate due to the presence of the magneto-rotational mechanism.

This paper is organised as follows: in Sect. 2 we discuss our model; Sect. 3 shortly recalls the model from Narayan et al. (2002); in Sect. 4 we present our results, including a comparison with the results from Narayan et al. (2002); and finally in Sect. 5 we present our conclusions.

2. Accretion disk model

2.1. Equilibrium of a differentially rotating plasma

We want to investigate the growth rate of instabilities occurring in a magnetized accretion disk. In order to quantify instabilities using a linear analysis, one has to consider an MHD equilibrium. In our case, this equilibrium is one of a differentially rotating plasma that is radially stratified. In our model the density, pressure, magnetic field strength, and toroidal velocity only depend on the radius r. This type of model is sometimes referred to as an accretion disk in the cylindrical limit (see for example Hawley 2001).

We use an equilibrium as in Blokland et al. (2005), generalised with an additional parameter a, which is introduced in order to allow for convective instabilities. The following profiles are used for density ρ, thermal pressure p, toroidal magnetic field B_θ, axial magnetic field B_z, and the toroidal velocity v_θ respectively:

$$\rho = r^{-(3+a)/2}, \tag{1}$$

$$p = \epsilon^2 \ r^{-(5+a)/2}, \tag{2}$$

$$B_\theta = -\alpha_1 \sqrt{\frac{2\epsilon^2}{\beta(\alpha_1^2+\alpha_2^2)}} \ r^{-(5+a)/4}, \tag{3}$$

$$B_z = \alpha_2 \sqrt{\frac{2\epsilon^2}{\beta(\alpha_1^2+\alpha_2^2)}} \ r^{-(5+a)/4}, \tag{4}$$

$$v_\theta = V_0 \ r^{-1/2}, \tag{5}$$

in which the α-parameters can be expressed as the ratio of both the toroidal and axial magnetic field over the total magnetic field B like

$$B_\theta/B = -\alpha_1/\sqrt{\alpha_1^2+\alpha_2^2}, \tag{6}$$

$$B_z/B = \alpha_2/\sqrt{\alpha_1^2+\alpha_2^2}, \tag{7}$$

and the parameter V_0 is defined as:

$$V_0^2 = GM_* - \frac{\epsilon^2}{2\beta\left(\alpha_1^2+\alpha_2^2\right)} \times \left((5+a)(1+\beta)\left(\alpha_1^2+\alpha_2^2\right) - 4\alpha_1^2\right). \tag{8}$$

Here, G and M_* denote the gravitational constant and the mass of the central object respectively. Finally, the parameter β denotes the radially constant ratio between the thermal pressure and total magnetic pressure $B^2/2$, i.e. $\beta \equiv 2p/B^2$.

The above power-law profiles satisfy the radial force balance equation in cylindrical coordinates:

$$\left[p + \frac{1}{2}B^2\right]' + \frac{B_\theta^2}{r} = \frac{\rho v_\theta^2}{r} - \rho g, \tag{9}$$

here g denotes GM_*/r^2, and the prime indicates the derivative with respect to radius r.

The differences between our equilibrium and the one in Narayan et al. (2002) are: 1) we *explicitly* define the above-mentioned equilibrium quantities by using power-law profiles as a function of radius r; 2) we include the toroidal magnetic field component B_θ; 3) we define a ratio of scale height H over radius r, i.e. $\epsilon \equiv H/r$, in order to quantify the thickness of our disk model; and 4) we do not exclude disks close to equipartition (β is a free parameter).

2.2. Determining the growth rate of instabilities

We use the local dispersion equation solver, which was recently discussed by Blokland et al. (2005). This code calculates the growth rate of the most unstable mode in a given MHD equilibrium for a given radial "wavenumber" (q), and a toroidal (m) and axial wavenumber (k) at a given position r_i. We will only consider axisymmetric perturbations ($m = 0$) in this paper.

In order to determine the radial "wavenumber" q, we use the method discussed by Blokland et al. (2005). It is shown there that under certain assumptions, the numerical solution of the full set of linearised compressible MHD equations governing all MHD modes in disk equilibria obeying Eq. (9) can be avoided for modes obeying a local dispersion equation found from WKB analysis. Excellent agreement between the growth rate and the eigenfunction behaviour was demonstrated when position r_i and associated "wavenumber" q were properly calculated from the full numerical solution. In this paper we follow Balbus & Hawley (1991) and Narayan et al. (2002), who effectively take $q = 0$, in order to make a direct comparison with their calculations. We notice that we only observed a difference on the order of 1% in our obtained growth rates with respect to our calculations, for which the "wavenumber" q was properly calculated.

The local dispersion equation solver finds the root of a sixth order polynomial using Laguerre's method (Press et al. 1988). This sixth order polynomial dispersion equation represents the local dispersion equation as an approximation to the true 10th degree WKB local dispersion equation (Blokland et al. 2005), which is more general than the one discussed by Narayan et al. (2002): 1) it allows calculation of the growth rate of instabilities for an equilibrium that has both an axial and a toroidal magnetic field component; and 2) the equilibrium can be either weakly magnetized or close to equipartition. Narayan et al. (2002) could not consider disks close to equipartition, because the fourth order polynomial from Balbus & Hawley (1991) was derived *assuming* a weak axial and no toroidal magnetic field component.

3. Accretion disks with convection

3.1. A thick accretion disk

One of the key parameters of our MHD equilibrium is the parameter ϵ, which is taken as a constant free parameter. This parameter was introduced by Shakura & Sunyaev (1973) in their model of geometrically thin accretion disks, which are Keplerian rotating. The physical interpretation of ϵ in these models is the same as in the MHD equilibrium we consider here, i.e. $\epsilon = c_s/v_\theta \simeq H/r$, where c_s denotes the sound speed. MRI instabilities in thin accretion disk models were considered by Blokland et al. (2005). However, in this paper we consider values of $\epsilon \sim 1$; i.e. we are in the regime of sub-Keplerian rotating disks (see e.g. Narayan & Yi 1994). For these cases we stick to the interpretation $\epsilon \simeq H/r$, noting that the identification $\epsilon = c_s/v_\theta$ is not valid anymore. Typically, c_s/v_θ in our models will be larger up to a maximum factor of order $\sim$10. As mentioned in Sect. 2, our MHD equilibrium is an example of an accretion disk model within the cylindrical limit. One has to realise that results from these type of models approximate the *interior* of a real height-dependent accretion disk. This approximation is correct as long as the axial wavenumber k is much larger than the inverse of the scale height H. Therefore the identity $k \gg 2\pi/(\epsilon r)$ has to be satisfied in our calculations in order to connect these results with the interior of an accretion disk.

3.2. Convective instabilities

As discussed in Sect. 2, Narayan et al. (2002) also considered an equilibrium of a differentially rotating plasma that only allows for a weak axial magnetic field component. Furthermore, their equilibrium quantities depend on radius r, but are not explicitly defined as power-laws obeying the radial force balance Eq. (9). Therefore, in order to introduce convective instabilities in their model, they describe the stratification of the differentially rotating plasma in terms of a free parameter N^2, which is directly related to the Brunt-Väisälä frequency $N_{\rm BV}$:

$$N^2 = -N_{\rm BV}^2 = \frac{3}{5\rho}\frac{{\rm d}p}{{\rm d}r}\frac{{\rm d}\ln\left(p\rho^{-5/3}\right)}{{\rm d}r}. \quad (10)$$

In a weakly-magnetized rotating medium, the onset of convection is determined by the Høiland criterium, i.e. $N^2 > \kappa^2(\equiv 2v_\theta(rv_\theta)'/r^2)$, where κ is the epicyclic frequency. Furthermore, they assume a purely Keplerian system, which means that $\kappa^2 = \Omega_{\rm K}^2$, therefore convective instabilities will be present in their model when $N^2 > \Omega^2$. Narayan et al. (2002) present growth rates of instabilities as a function of the axial wavenumber. They use the equation for the growth rate derived by Balbus & Hawley (1991). They normalise their obtained growth rates to the rotational frequency; furthermore, the wavevector is multiplied by the Alfvén velocity $V_{\rm A}$, and also normalised to the rotational frequency. In this way the only free parameter left for the growth rate profiles is the parameter N^2/Ω^2. Figure 1 shows these scaled growth rates for the different values of N^2/Ω^2 considered by Narayan et al. (2002).

In our cylindrical accretion disk model with power-law equilibrium profiles one can calculate N^2/Ω^2, and make a direct comparison with the work of Narayan et al. (2002). Furthermore, it can be shown that in our MHD equilibrium the equality $\kappa^2 = \Omega^2$ is always valid, even if the system is not Keplerian rotating (i.e. when $\epsilon \sim 1$). Therefore our MHD equilibrium will also be convectively unstable once $N^2 > \Omega^2$, as in the model from Narayan et al. (2002), the difference being that our model captures significant deviations from *Keplerian rotating* disks by means of the ϵ parameter ($\Omega^2 \neq \Omega_{\rm K}^2$).

The Høiland criterium is valid for a hydrodynamical equilibrium, but strictly speaking it is not valid for an MHD equilibrium, which is weakly magnetized. However, it can be used as an indication of convective instabilities at those wavenumbers where the restoring magnetic tension force is much smaller than the buoyancy force (see also Christodoulou et al. 2003). These authors derive a stability criterium for axial perturbations for magnetized equilibria with purely toroidal magnetic fields. This criterium is valid for all values of the plasma parameter β, which therefore includes equilibria that are weakly magnetized or close to equipartition. Therefore this criterium could be used to determine the presence of convective instabilities in our models with purely toroidal magnetic fields. The criterium can also be derived from the local dispersion equation (see e.g. Keppens et al. 2002; Blokland et al. 2005; Wang et al. 2004).

3.3. A model for the interior of a thick accretion disk

In our MHD equilibrium, the parameter ϵ is a free parameter to be interpreted as related to the scale-height H at each radial position r. In order to perform a meaningful stability calculation for an accretion disk, the wavenumbers of the unstable modes considered must be such that they are able to manifest themselves in the *interior* of the accretion disk. These instabilities *fit* into the interior of the considered accretion disk model once the corresponding axial wavenumber $k > k_{\rm min} \equiv 2\pi/H$. Analysis by Narayan et al. (2002) shows a maximum of the growth rate at $\log(kV_{\rm A}/\Omega) \sim 0.0$ (see Fig. 1). We therefore choose our MHD equilibria such that the numerical value of $\log(k_{\rm min}V_{\rm A}/\Omega)$ is typically less then ~ -1.5. For these models, all unstable modes found with an axial wavenumber $k > k_{\rm min}$ *fit* into the interior of the considered disk model, and include the most unstable ones.

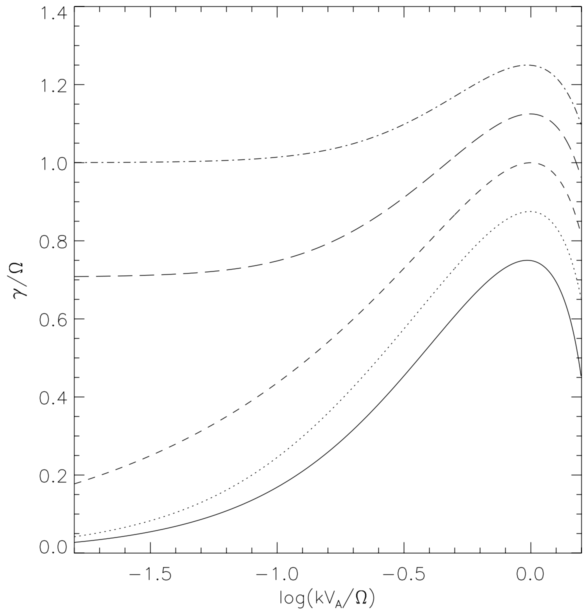

Fig. 1. Dimensionless growth rate γ/Ω as a function of dimensionless wavevector kv_A/Ω for accretion disk models from Narayan et al. (2002). The five growth rates shown are from five different solutions: $N^2/\Omega^2 = 0.0$ (solid line); $N^2/\Omega^2 = 0.5$ (dotted line); $N^2/\Omega^2 = 1.0$ (short-dashed line); $N^2/\Omega^2 = 1.5$ (long-dashed line); $N^2/\Omega^2 = 2.0$ (dot-dashed line).

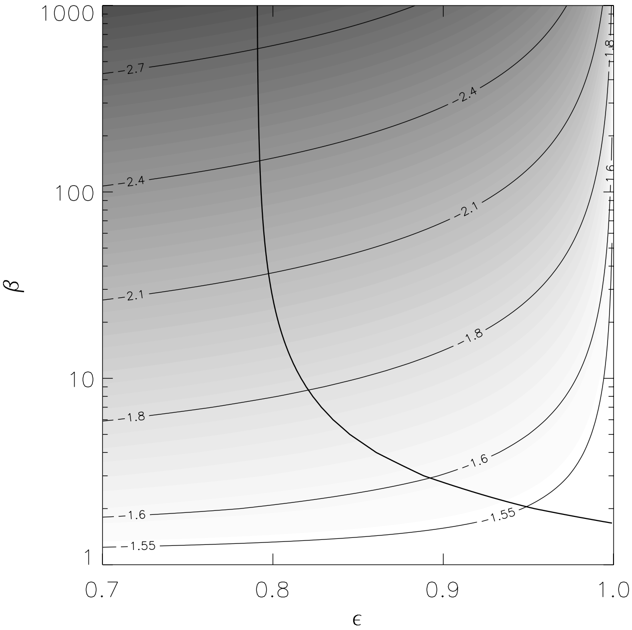

Fig. 2. Logarithmic gray-scale plot of the value $\log(k_{\min}V_A/\Omega)$ in the model for which $\alpha_1 = 300.0, \alpha_2 = 1.0$, and $a = -3.0$. The solid thick line corresponds to $N^2 = \Omega^2$. The thick solid curve for the Høiland criterium deviates from a straight vertical line, because of the *dynamical importance* of the magnetic field on the equilibrium for low values of β.

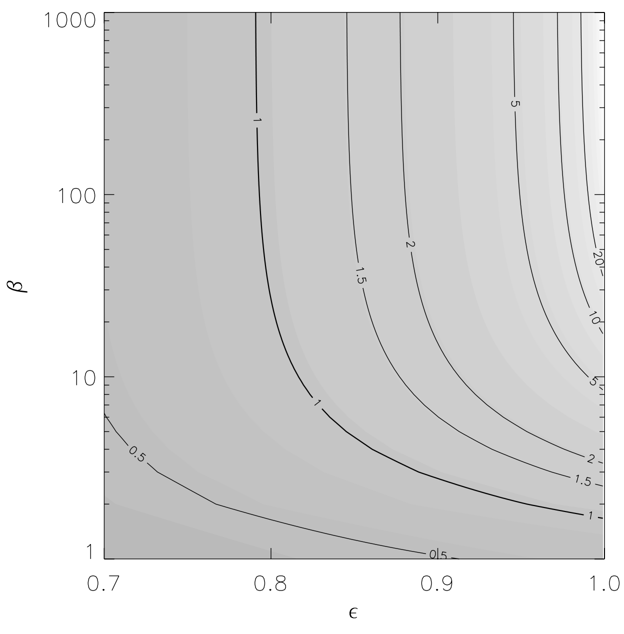

Fig. 3. Gray-scale plot of the parameter N^2/Ω^2 in the model for which $\alpha_1 = 300.0, \alpha_2 = 1.0$ and $a = -3.0$.

We found that in order to satisfy the restriction $k > k_{\min}$ with $\log(k_{\min}V_A/\Omega) \sim -1.5$ a high ratio of the toroidal magnetic field strength to the axial magnetic field strength is needed. Figure 2 shows the parameter log $(k_{\min}V_A/\Omega)$ as a function of the parameters ϵ and β of our model, for which the other parameters have been fixed. Indeed for most values of ϵ and β the corresponding numerical value log $(k_{\min}V_A/\Omega) < -1.5$. The thick solid line in Fig. 2 marks the Høiland criterium, i.e. $N^2 = \Omega^2$. The models on the right hand side of this line are convectively unstable, while the models on the left hand side are convectively stable. Notice that the line $N^2 = \Omega^2$ can be drawn uniquely as a function of β and ϵ, once α_1 and α_2 are determined. This is because the numerical value of N^2/Ω^2, calculated from the equilibrium presented in Sect. 2, does not depend on radius r.

As argued above we will choose a configuration of an accretion disk with most of the magnetic field strength in the toroidal component, in order to allow for both convective and magneto-rotational instabilities. The values of the ratio of the Brunt-Väisälä frequency and the rotational frequency marks the free parameter in the paper by Narayan et al. (2002). We plot the numerical value of this parameter in our models in Fig. 3 and plot contours with $N^2/\Omega^2 = 0.5, 1.0, 1.5, 2.0$, corresponding to the models discussed in Narayan et al.(2002). Note that in very weakly magnetized, thick disk models we obtain high values for N^2/Ω^2, the highest value being $N^2/\Omega^2 = 600$ (model A in Table 1). Those are expected to be rigorously convective in a pure hydrodynamical sense.

4. Accretion disks with two instabilities

4.1. Introduction

We present the results from a linear analysis performed for different MHD equilibria, using the local dispersion equation solver. Our calculations only considered equilibria with constant density ($a = -3.0$), while most of the magnetic field

Table 1. Parameters of accretion disk models: all the models considered have $\alpha_1 = 300$, $a = -3$ and $\alpha_2 = 1$ ($\alpha_2 = 0$) for models with (without) axial magnetic field.

Sim	ϵ	β	N^2/Ω^2
A	1.0	1000.0	600.0
B	0.94	1000.0	4.5
C	0.88	1000.0	2.0
D	0.845	1000.0	1.5
E	1.0	20.0	12.0
F	1.0	10.0	6.0

strength is in the toroidal direction ($\alpha_1 = 300.0$; $\alpha_2 = 1.0$). Finally, we only considered thick accretion disk models by considering MHD equilibria with $\epsilon \geq 0.8$, in order to allow for mixed convective magneto-rotational instabilities. We considered five different MHD equilibria and calculate the growth rates of the unstable modes. Additionally, we repeat these calculations for all five models with the only difference being that the axial magnetic field equals zero ($\alpha_2 = 0.0$). Since we are only considering axisymmetric perturbations, these last calculations yield instabilities that cannot have a magneto-rotational nature and are purely convective instabilities. Because the axial magnetic fields are weak, comparing the growth rates of the same model with and without the axial magnetic field component provides a quantitative measure of the magneto-rotational contribution of an unstable mode in the interior of an accretion disk.

4.2. Weakly magnetized disks: from sub-Keplerian to near-Keplerian disks

In this subsection, we investigate the influence of the parameter ϵ on the nature of the instabilities in weakly magnetized ($\beta = 1000$) MHD equilibria (models A–D, Table 1). We present the growth rates of the instabilities in our model as a function of the axial wavenumber, using the same scaling as Narayan et al. (2002).

Figure 4 shows our results for model A, which has a corresponding value of the ratio $N^2/\Omega^2 = 600$ (model A, Table 1). The left panel shows a comparison between our calculations for the growth rate of the instabilities (crosses) and those of Narayan et al. (2002) (solid line). There is perfect agreement between both results. The right panel shows the ratio of the growth rate of model A with an axial magnetic field ($\alpha_2 = 1.0$) with respect to model A without an axial magnetic field ($\alpha_2 = 0.0$). The model without axial magnetic field excludes the magneto-rotational mechanism completely. One can see that the ratio never exceeds unity, implying that there is no enhancement of the growth rate due to the magneto-rotational mechanism. Furthermore, we observe in the left and right panels that there is no observed maximum value of the growth rate at $\log(kv_{\rm A}/\Omega) \approx 0.0$, a feature also associated with the magneto-rotational instability. Therefore, the observed instabilities have a (nearly) completely convective nature in this particular disk model, as expected from the very high value of N^2/Ω^2.

Figure 5 shows our results for model B, which has a corresponding value of the ratio $N^2/\Omega^2 = 4.5$ (model B, Table 1). One can see in the left panel that the growth rate from our calculations (crosses) again matches the solution for the growth rate (solid line) in Narayan et al. (2002), despite the fact that we consider an overall weak, but predominantly toroidal magnetic field. The right panel of Fig. 5 shows the ratio of the growth rate of model B with axial magnetic field ($\alpha_2 = 1.0$), with respect to model B without an axial magnetic field component ($\alpha_2 = 0.0$). It is observed that there is an overall small contribution (less than 1 percent) to the growth rates by the magneto-rotational mechanism. This indicates that the unstable modes have a dominant convective nature in this model, like in model A.

In model C, the thickness of the disk model was reduced further, such that the obtained ratio $N^2/\Omega^2 \simeq 2.0$ equals the maximum value Narayan et al. (2002) have considered in their paper. The left panel of Fig. 6 shows the calculated growth rates (crosses) of this MHD equilibrium, and there is a perfect match with the solution (solid line) in Narayan et al. (2002). The right panel of Fig. 6 shows the ratio of the growth rate of model C with axial magnetic field ($\alpha_2 = 1.0$) with respect to model C without an axial magnetic field component ($\alpha_2 = 0.0$). The contribution from the magneto-rotational mechanism is significant, approximately 25 percent at values of the wavenumber where the growth rate has its maximum, an increase that indicates that the unstable modes in this range of wavenumbers are significantly amplified by the magneto-rotational mechanism. Furthermore, model C shows that for axial wavenumbers $\log(kv_{\rm A}/\Omega) < -1.0$, the contribution of the magneto-rotational mechanism has decreased to a few percent. This indicates that the unstable modes in this range of wavenumbers have a dominant convective nature. This conclusion about the long wavelength regime was also made by Narayan et al. (2002) in their analysis.

Finally, Fig. 7 shows our results for model D, which has a corresponding value of the ratio $N^2/\Omega^2 = 1.5$ (see Table 1). The left panel of Fig. 7 shows the calculated growth rates (crosses) of this MHD equilibrium, in agreement with the solution (solid line) in Narayan et al. (2002). The right panel of Fig. 7 shows the ratio of the growth rate of model D with axial magnetic field ($\alpha_2 = 1.0$) with respect to model D without an axial magnetic field component ($\alpha_2 = 0.0$). The contribution from the magneto-rotational mechanism increases up to 60 percent around values of the wavenumber where the growth rate has its maximum. For axial wavenumbers $\log(kv_{\rm A}/\Omega) < -1.0$, the contribution of the magneto-rotational mechanism has a maximum of about 5 percent, which indicates their dominant convective nature.

Models C and D discussed above have the same ratio of N^2/Ω^2 as the models discussed by Narayan et al. (2002). Our conclusions confirm those by Narayan et al. (2002) for the unstable long-wavelength modes ($kV_{\rm A} \ll \Omega$) in these two models: they are clearly convective modes. However, the wavelength modes in these models with $kV_{\rm A} \sim \Omega$ are shown to be maximally amplified by the magneto-rotational mechanism. The amplification increases as the ratio N^2/Ω^2 decreases.

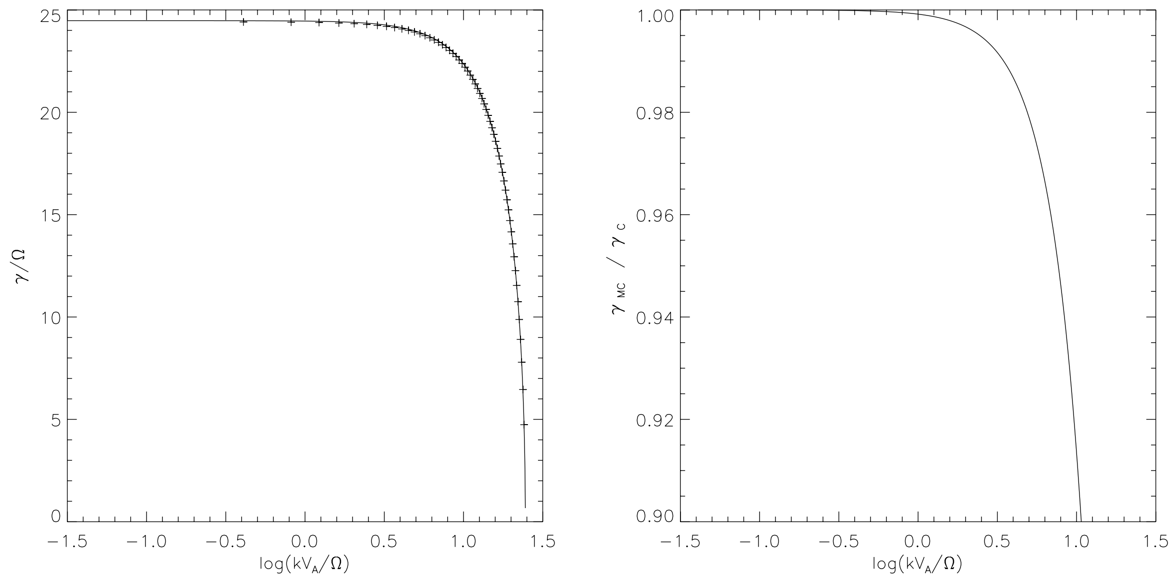

Fig. 4. *Left panel*: dimensionless growth rate γ/Ω as a function of dimensionless wavenumber $kv_{\rm A}/\Omega$ for MHD equilibrium A (see Table 1). The solid line corresponds to the solution from Narayan et al. (1994). The crosses correspond to the solution using the code LODES. *Right panel*: ratio of the growth rate $\gamma_{\rm MC}$ with ($\alpha_2 = 1.0$) and the growth rate $\gamma_{\rm C}$ without ($\alpha_2 = 0.0$) an axial magnetic field component as a function of the dimensionless wavenumber $kv_{\rm A}/\Omega$.

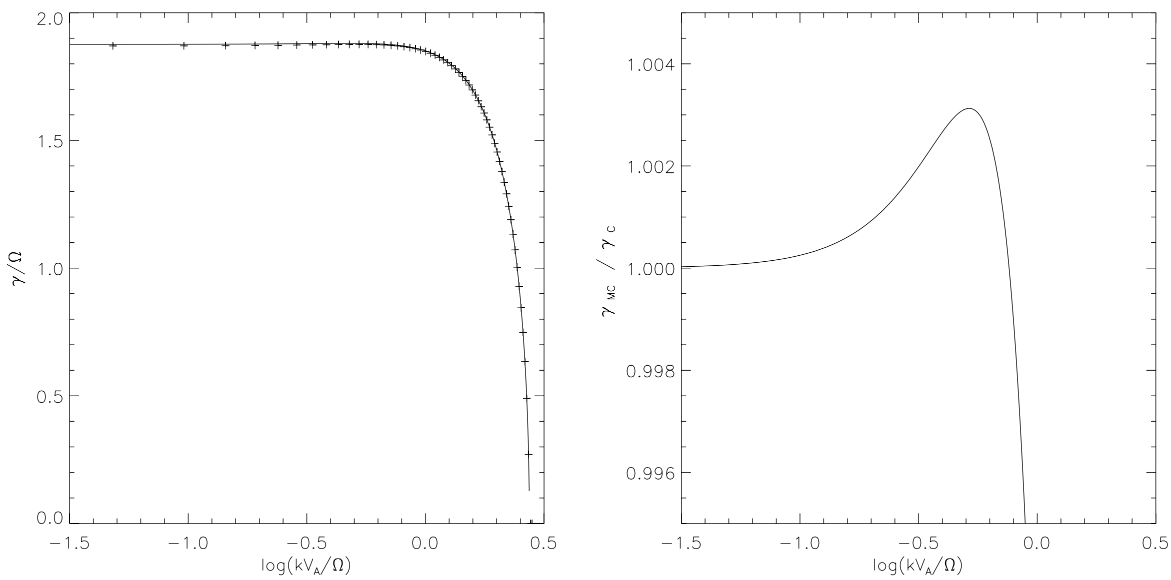

Fig. 5. *Left panel*: dimensionless growth rate γ/Ω as a function of dimensionless wavenumber $kv_{\rm A}/\Omega$ for MHD equilibrium B (see Table 1). The solid line corresponds to the solution by Narayan et al. (1994). The crosses correspond to the solution using the code LODES. *Right panel*: ratio of the growth rate $\gamma_{\rm MC}$ with ($\alpha_2 = 1.0$) and the growth rate $\gamma_{\rm C}$ without ($\alpha_2 = 0.0$) an axial magnetic field component as a function of the dimensionless wavenumber $kv_{\rm A}/\Omega$.

However, these modes seem to be determined by both the convective and the magneto-rotational mechanism. Finally, for modes with $kV_{\rm A} > \Omega$, amplification of the growth rate is shown to be decreasing, due to the restoring magnetic tension force.

4.3. From weakly magnetized disks to disks close to equipartition

In this subsection we investigate the influence of the magnetization on the nature of the instabilities in our considered MHD equilibria (models E and F, Table 1).

Figure 8 shows our results for model E. The considered MHD equilibrium has the same parameters as model A from the previous subsection, except this one is closer to equipartition ($\beta = 20$). Due to the stronger magnetic field, this equilibrium has a lower value for the ratio N^2/Ω^2 (see Table 1). Our calculations (crosses) and the calculation by Narayan et al. (2002) (solid line) deviate from each other, since the equation used by Narayan et al. (2002) is not valid for this model. This is because the toroidal magnetic field strength cannot be neglected anymore in the linear analysis, a component which was not taken into account in the equation used by

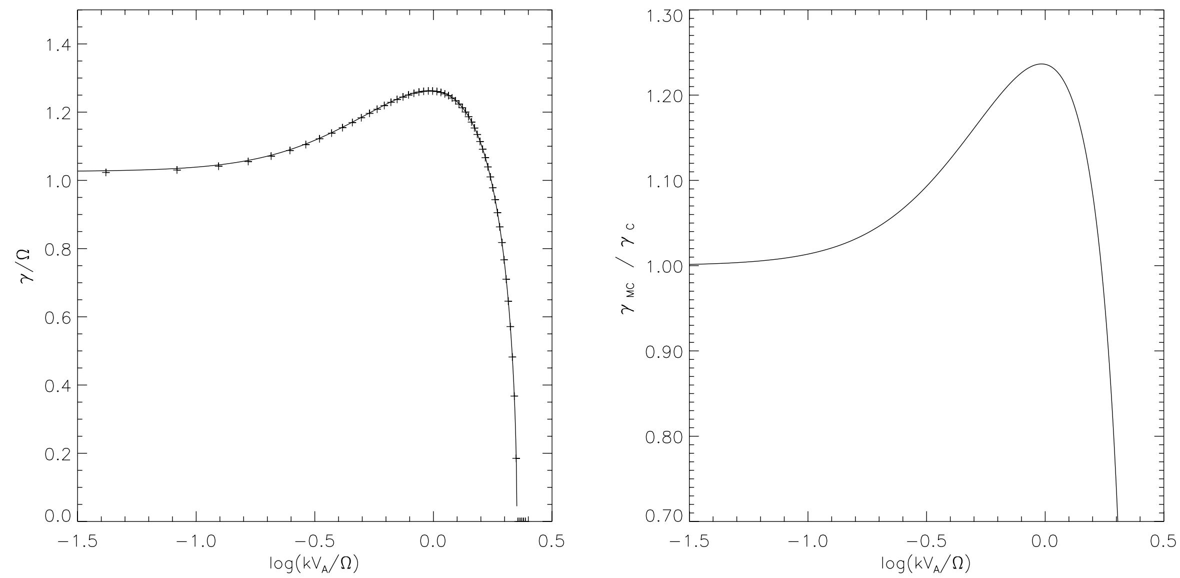

Fig. 6. *Left panel*: dimensionless growth rate γ/Ω as a function of dimensionless wavenumber kv_{A}/Ω for MHD equilibrium C (see Table 1). The solid line corresponds to the solution by Narayan et al. (1994). The crosses correspond to the solution using the code LODES. *Right panel*: ratio of the growth rate γ_{MC} with ($\alpha_2 = 1.0$) and the growth rate γ_{C} without ($\alpha_2 = 0.0$) an axial magnetic field component as a function of the dimensionless wavenumber kv_{A}/Ω.

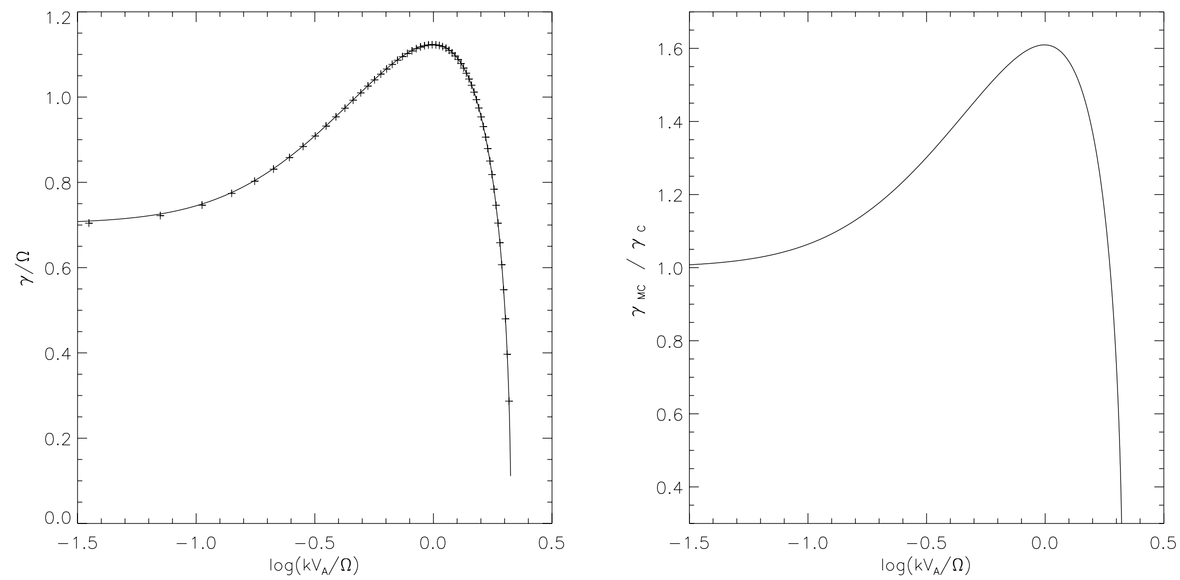

Fig. 7. *Left panel*: dimensionless growth rate γ/Ω as a function of dimensionless wavenumber kv_{A}/Ω for MHD equilibrium D (see Table 1). The solid line corresponds to the solution by Narayan et al. (1994). The crosses correspond to the solution using the code LODES. *Right panel*: ratio of the growth rate γ_{MC} with ($\alpha_2 = 1.0$) and the growth rate γ_{C} without ($\alpha_2 = 0.0$) an axial magnetic field component as a function of the dimensionless wavenumber kv_{A}/Ω.

Narayan et al. (2005). In contrast to model A, this model shows a maximum value for the growth rate, close to the typical value of the magneto-rotational instability, i.e. $\log(kv_{\mathrm{A}}/\Omega) \approx 0.0$. The right panel shows the ratio of the growth rate of model E with axial magnetic field ($\alpha_2 = 1.0$) with respect to model E without an axial magnetic field component ($\alpha_2 = 0.0$). There is a slight enhancement observed close to the maximum value of the growth rate, which indicates that the magneto-rotational mechanism starts to contribute to the growth rate of unstable modes in this region. Notice that the enhancement is still very weak, approximately 1 percent (right panel Fig. 8).

Finally, Fig. 9 shows our results for model F. In this MHD equilibrium the magnetization is close to equipartition ($\beta = 10.0$), with a corresponding value $N^2/\Omega^2 = 6.0$ (see Table 1). We do not consider a disk in exact equipartition (i.e. $\beta = 1.0$), because this model would not allow for convective instabilities (i.e. $N^2/\Omega^2 < 1$ as can be seen in Fig. 3). The left panel of Fig. 9 shows that the approximation by Narayan et al. (2002) (solid line) is no longer valid. Taking the toroidal magnetic field component into account, our calculations show a distinct maximum, which occurs at the typical value $\log(kv_{\mathrm{A}}/\Omega) = 0.0$ for magneto-rotational instabilities. The right panel of Fig. 9

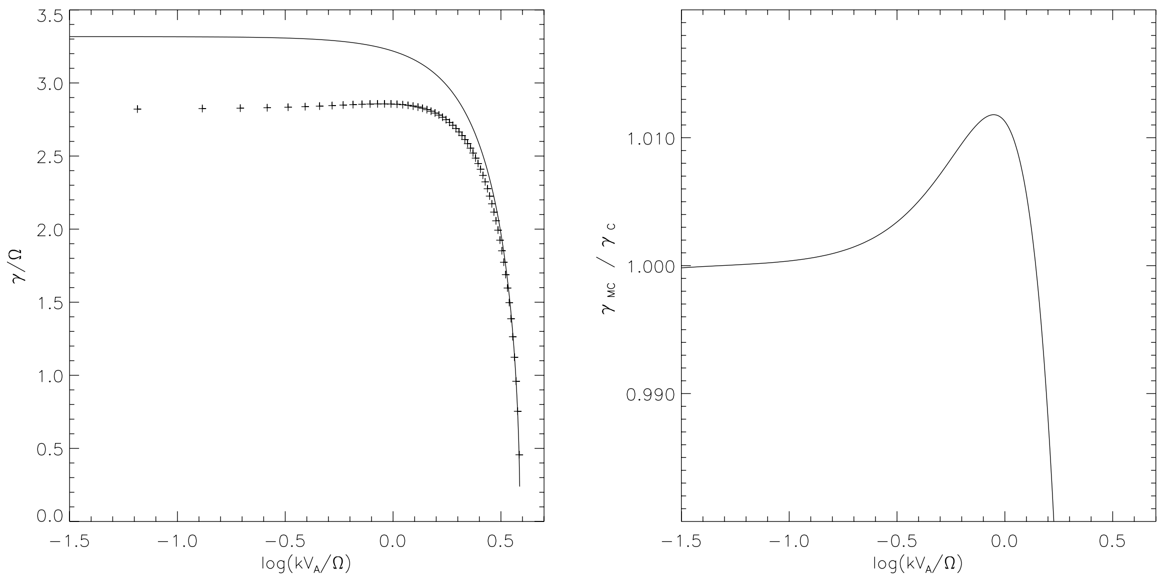

Fig. 8. *Left panel*: dimensionless growth rate γ/Ω as a function of dimensionless wavenumber $kv_{\rm A}/\Omega$ for MHD equilibrium E (see Table 1). The solid line corresponds to the solution by Narayan et al. (1994). The crosses correspond to the solution using the code LODES. *Right panel*: ratio of the growth rate $\gamma_{\rm MC}$ with ($\alpha_2 = 1.0$) and the growth rate $\gamma_{\rm C}$ without ($\alpha_2 = 0.0$) an axial magnetic field component as a function of the dimensionless wavenumber $kv_{\rm A}/\Omega$.

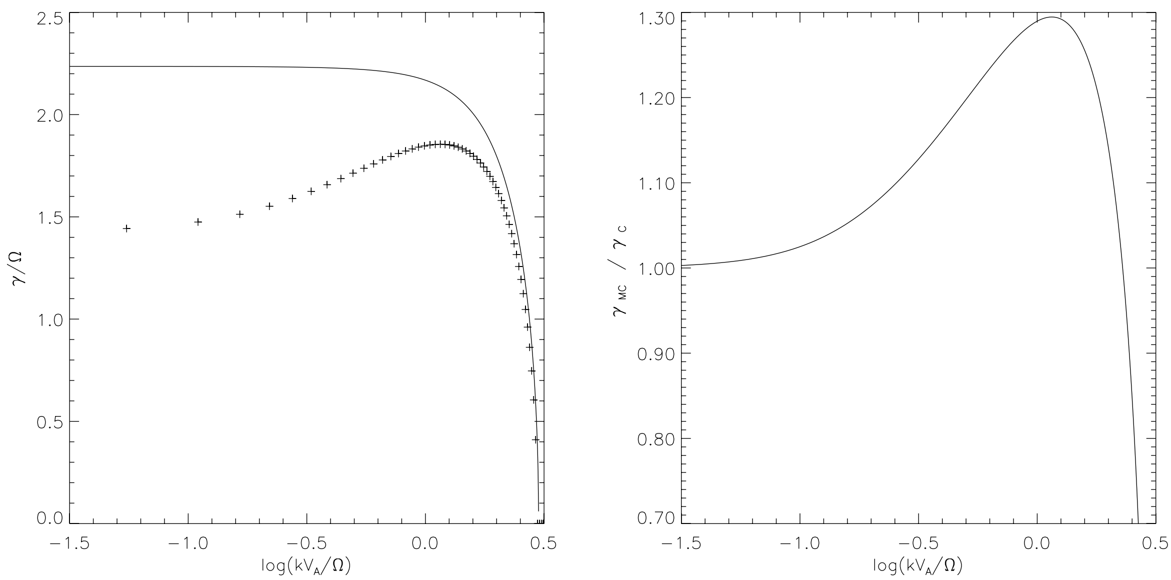

Fig. 9. *Left panel*: dimensionless growth rate γ/Ω as a function of dimensionless wavenumber $kv_{\rm A}/\Omega$ for MHD equilibrium F (see Table 1). The solid line corresponds to the solution by Narayan et al. (1994). The crosses correspond to the solution using the code LODES. *Right panel*: ratio of the growth rate $\gamma_{\rm MC}$ with ($\alpha_2 = 1.0$) and the growth rate $\gamma_{\rm C}$ without ($\alpha_2 = 0.0$) an axial magnetic field component as a function of the dimensionless wavenumber $kv_{\rm A}/\Omega$.

shows the ratio of the growth rate of model F with axial magnetic field ($\alpha_2 = 1.0$) with respect to model F without an axial magnetic field component ($\alpha_2 = 0.0$). It can be observed that in the region around the maximum of the growth rate, the contribution of the magneto-rotational mechanism is approximately 30 percent. This increase indicates that the unstable modes in this range of wavenumbers are significantly amplified by the magneto-rotational mechanism. However, for axial wavenumbers $\log(kv_{\rm A}/\Omega) < -1.0$, the contribution of the magneto-rotational mechanism has decreased to a few percent, which indicates that the unstable modes in this range of wavenumbers have a dominant convective nature.

5. Conclusions

We calculated growth rates of instabilities for MHD equilibria of magnetized accretion disks. The disks models were taken within the cylindrical limit and included both toroidal and axial magnetic field components. Due to the presence of a toroidal magnetic field component, the unstable modes we find are strictly speaking *overstable* modes (see e.g. Blokland et al. 2005). The parameters of the model in our calculations were taken such that the axial wavenumber of the most unstable modes was larger than the inversed scale height H. Therefore the analysis can be used as an approximation for a stability analysis of the interior of an accretion disk. Our models considered both weakly magnetized disks, as well as disks which are close to equipartition. All calculations were performed with a restriction to axisymmetric perturbations ($m = 0$).

Our most important results are summarised below:

- We have considered models of thick accretion disks that are subject to convective magneto-rotational instabilities, and we quantified the contribution of the MRI mechanism for all the instabilities considered.
- Our calculations diverge from the solutions by Narayan et al. (2002), when the disk models become significantly magnetized. The deviations are contributed to the toroidal magnetic field component, which was neglected in the derivation of the equation for the growth rate used by Narayan et al. (2002).
- Our calculations show that the contribution from the magneto-rotational mechanism to the growth rate becomes significant as the disks get close to equipartition. The contribution peaks for modes near the maximum value of the growth rate.
- Our calculations for the growth rates agree with those of Narayan et al. (2002) for weakly magnetized accretion disk models, even though we include dominant toroidal field components.
- Our calculations show that the contribution from the magneto-rotational mechanism to the growth rate becomes significant as the scale-height H is decreased. This contribution peaks for modes near the maximum value of the growth rate.
- All our calculations show that the contribution from the magneto-rotational mechanism to the growth rate becomes neglible for unstable modes with $\log(kv_A/\Omega) < -1.0$, which are safely interpreted as purely convective modes in all cases.

Acknowledgements. J.W.B. and R.K. carried out this work within the framework of the European Fusion Programme, and it is supported by the European Communities under the contract of Association between EURATOM/FOM. Views and opinions expressed herein do not necessarily reflect those of the European Commission. EvdS did this research in the FOM projectruimte on "Magnetoseismology of accretion disks", a collaborative project between R. Keppens (FOM Institute Rijnhuizen, Nieuwegein) and N. Langer (Astronomical Institute Utrecht). This work is part of the research programme of the "Stichting voor Fundamenteel Onderzoek der Materie (FOM)", which is financially supported by the "Nederlandse Organisatie voor Wetenschappelijk Onderzoek (NWO)".

References

Baganoff, F. K., Bautz, M. W., Brandt, W. N., et al. 2001, Nature, 413, 45
Balbus, S. A., & Hawley, F. H. 1991, ApJ, 376, 214
Balbus, S. A., & Hawley, F. H. 2002, ApJ, 573, 749
Blokland, J. W. S., van der Swaluw, E., Keppens, R., & Goedbloed, J. P. 2005, A&A, 444, 337
Christodoulou, D. M., Contopoulos, J., & Kazanas, D. 2003, ApJ, 586, 372
Di Matteo, T., Allen, S. W., Fabian, A. C., Wilson, A. S., & Young, A. J. 2003, Ap, 582, 133
Hawley, J. F. 2001, ApJ, 554, 534
Keppens, R., Casse, F., & Goedbloed, J. P. 2002, ApJ, 569, L121
Narayan, R., & Yi, I. 1994, ApJ, 428, L13
Narayan, R., Quataert, I. V., Igumenshchev, I. V., & Abramowicz, M. A. 2002, ApJ, 577, 295
Press, W. H., Teukolsky, S. A., Vetterling, W. T., & Flannery, B. P. 1988, Numerical Recipes (New York: Cambridge Univ. Press)
Shakura, N. I., & Sunyaev, R. A. 1973, A&A, 24, 337
Tassoul, J. L. 1987, Theory of Rotating Stars (Princeton University Press)
Wang, C., Blokland, J. W. S., Keppens, R., & Goedbloed, J. P. 2004, J. Plasma Phys. 70(6), 651